Journal of Organometallic Chemistry 752 (2014) 6–11

Contents lists available at ScienceDirect

Journal of Organometallic Chemistry

journal homepage: www.elsevier.com/locate/jorganchem

Synthesis and photophysical properties of platinum(II) arylacetylides with donor–acceptor structures

Denghui Yao [a], Haiping Wang [a], Jin Guo [b], Tingfeng Wang [b], Liying Zhang [a], Junfeng Shao [b], Fengqi Guo [a,*]

[a] College of Chemistry and Molecular Engineering, Zhengzhou University, Zhengzhou 450001, PR China
[b] State Key Laboratory of Laser Interaction with Matter, Changchun Institute of Optics, Fine Mechanics and Physics, Chinese Academy of Sciences, Changchun 130033, PR China

ARTICLE INFO

Article history:
Received 26 September 2013
Received in revised form
18 November 2013
Accepted 23 November 2013

Keywords:
Platinum(II)
Arylacetylides
Nonlinear
Photophysical

ABSTRACT

The detailed relationship between the structure and the nonlinear mechanisms, as well as whether different nonlinear mechanisms of an organic molecule restrain each other are still not clear. In this paper, eight platinum(II) arylacetylides with donor–acceptor structures were synthesized and their photophysical properties were studied systematically. The properties of HOMO and LUMO were calculated using DFT method, the contribution of the metal d_π and charge transfer process are dominated by the skeleton structure of these complexes. The ligand-to-metal charge transfer (LMCT) happens when the molecule with D–π–Pt–π–D or D–π–Pt–π–Ar–π–Pt–π–D skeleton is excited, however the metal-to-ligand charge transfer (MLCT) and ligand-to-ligand charge transfer (LLCT) happen when the molecule with D–π–Pt–π–A, A–π–Pt–π–A or A–π–Pt–π–Ar–π–Pt–π–A skeleton is excited, respectively. The weak absorption in the visible area of these molecules provides a wide observation window for the application in optical limiter. The low fluorescent quantum yields and detectable room temperature phosphorescence indicate that the system-cross quantum yields of the title complexes containing Pt(II) is effective because of the spin-orbit coupling between the d orbitals of the Pt(II) and the large π-conjugated system. The first-order polarizabilities $|\beta_{xxx}|$ was determined by the solvatochromic method between 1.02×10^{-29} to 3.46×10^{-28} (cm^5/esu).

1. Introduction

Organic and organometallic materials with large nonlinear optical properties have been attracting great interests in the last two decades due to their potential applications in optical limiting, photodynamic therapy, and optical data storage, in which the two-photon absorption and excited state absorption are the two most important mechanisms [1–6]. A significant conclusion from the previous work could be made that the molecules with donor (D)–acceptor (A) structures, such as D–A, D–A–D, D–π–A, D–π–D, D–π–A–π–D and A–π–D–π–A, generally exhibit excellent two-photon absorption properties, and the two-photon absorption cross sections can be increased by extending the molecular conjugated system [7,8]. In addition, molecules containing heavy metal ions and rigid structure always exhibit large reverse saturable absorption due to the enhancement of the intersystem crossing from the first singlet excited state to the first triplet excited state [9–11]. These conclusions can provide helpful guidelines for designing materials with large nonlinear optical properties.

Platinum acetylide oligomers and polymers exhibit high linear transmission and strong reverse saturable absorption from visible to infrared spectral region because of the spin–orbit coupling interaction between the d orbitals of the heavy metal Pt(II) ion and the large π-conjugated system [11–13]. The two-photon absorption phenomenon of several platinum acetylide oligomers has also been reported recently, and the enhanced nonlinear absorption based on the absorption from both the singlet and triplet states also have been confirmed [14–17]. Although some papers have reported the relationship between the structure and reverse saturable absorption properties for the ns laser [11,13,18], or the two-photon absorption properties for ps laser [14,15], or the triplet–triplet upconversion properties [19,20] of platinum acetylide oligomers and polymers, respectively, the detailed relationship between the structure, the two-photon absorption and excited state absorption of the organic molecules are still not discussed clearly. Especially, whether the two-photon absorption and the excited state absorption of an organic molecule restrain each other is also not discussed

* Corresponding author. Tel.: +86 371 67739186.
E-mail address: fqguo@zzu.edu.cn (F. Guo).

0022-328X/$ – see front matter © 2013 Elsevier B.V. All rights reserved.
http://dx.doi.org/10.1016/j.jorganchem.2013.11.032

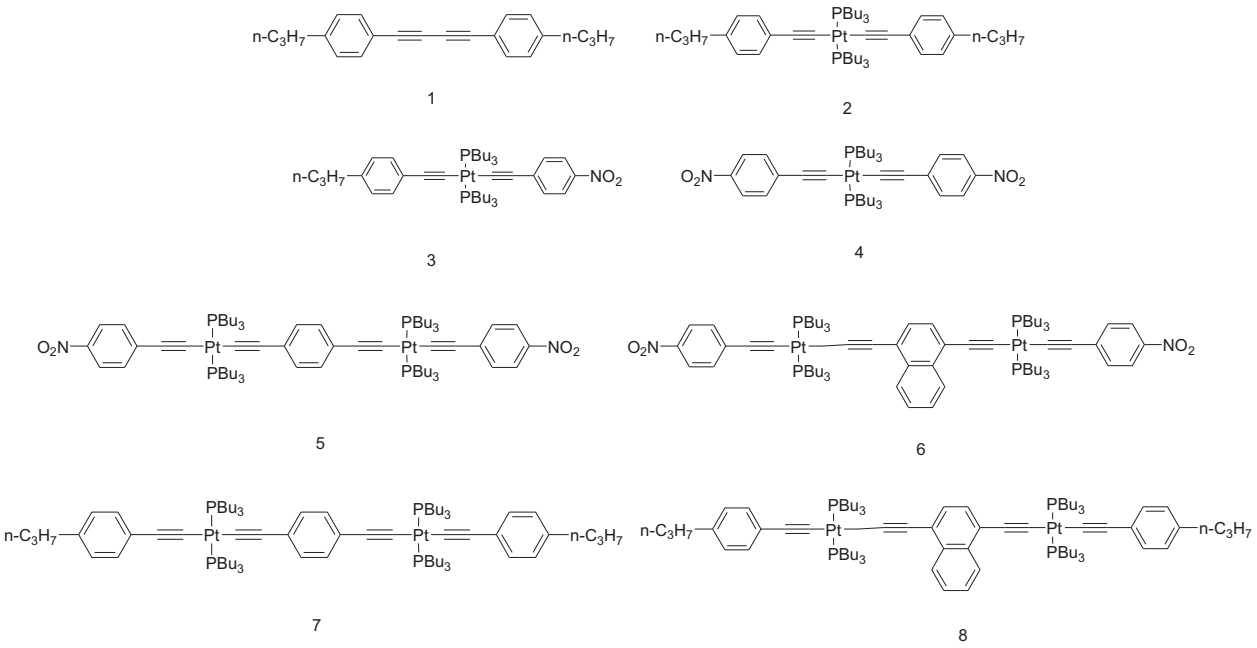

Fig. 1. Structures of the synthesized platinum acetylide oligomers with donor–acceptor structures.

deeply up to now. So it is necessary and important to address these questions for design nonlinear optical materials.

In this paper, a series of symmetric and unsymmetrical platinum acetylides with donor–acceptor structures, as shown in Fig. 1, were designed and synthesized. The design of complexes **1** to **4** is based on the well-known A–π–A, D–π–A and D–π–D motifs yielding materials with significant two-photon absorption, and the insertion of the heavy metal atom into an organic molecule often yields materials with strong excited state absorption from the triplet state. The synthesized platinum acetylides combine the donor–acceptor structure and heavy metal in one molecule, which make it possible to study the interaction between the two-photon absorption and excited state absorption related to the structure of the organic molecules. The component of metal and the conjugated length of the complexes **5** to **8** are increased in comparison with complexes **1** to **4**. The increase of the component of the metal should increase the intersystem crossing efficient of the molecule, this is helpful to understand the relationship between the excited absorption from the triplet state and the two-photon absorption, as well as how the two nonlinear optical properties restrain each other. This paper describes the synthesis processes and the detailed studies of the photophysical properties of the designed molecules.

2. Materials and methods

^{1}HNMR spectra were recorded on a DRX-400 spectrometer and the chemical shifts are reported relative to TMS. MALDI-TOF mass spectra were recorded on Autoflex III system. Elemental analyses were performed on a Flash EA 1112 Analyzer. Electronic absorption spectra were obtained on a UV-5200 spectrophotometer. Luminescence spectra were collected with a CaryEclipse fluorescence spectrometer. Fluorescence quantum yield and phosphorescence quantum yield were determined relative to the fluorescence standard compound quinine sulfate ($\Phi_{em} = 0.55$ at 313 nm excitation) [21] and phosphorescence stand complex $[Ru(bpy)_3]Cl_2$ ($\Phi_{em} = 0.042$ at 436 nm excitation) [22]. Lifetimes were measured on a FM-4P-TCSPC time-resolved fluorescence spectrometer.

All the starting materials were purchased from commercial available sources and used without any purification. All the solvents were dried and distilled by the standard methods. The initial arylacetylenes were synthesized from the corresponding aryl bromides and 2-methylbut-3-yn-2-ol via Sonagashira coupling reaction according to the literature [23–26]. *Trans*-$[Pt(PBu_3)_2Cl_2]$ was synthesized according to the literature method [27].

3. Result and discussion

3.1. Quantum calculation

The geometry of the platinum acetylides **2**, **3**, **4**, **5** and **7** were optimized and the HOMO and LUMO were calculated using the density functional theory (DFT) at 6-31G(d) level for C, H, N, O, P and Lanl2DZ level for Pt atoms, respectively. All the butyl groups in the molecules were replaced by the methyl groups in order to simplify the calculation process. The calculations were performed with the Gaussian 03 software [28]. The calculated electronic distribution situation is shown in Fig. 2 and the calculated energy of HOMO and LUMO are listed in table 1.

As shown in Fig. 2, the electronic density of the HOMO of **2** with symmetrical D–π–Pt–π–D skeleton is spread uniformly on the molecule, whereas the electronic density of the LUMO orbital is mostly located at the center of the molecule. An obvious ligand-to-metal charge transfer (LMCT) happens when molecule is excited, and the contribution of the metal d_π in LUMO is much higher than that in HOMO. The similar result is collected for **7**. The electronic density of the HOMO of **3** with unsymmetrical D–π–Pt–π–A skeleton is located at the donor side, whereas the electronic density of LUMO orbital is mostly located at the acceptor side. An obvious ligand-to-ligand charge transfer (LLCT) happens when the molecule is excited, and the contribution of the metal d_π in LUMO is lower than that in HOMO. The electronic density of the HOMO of **4** with symmetrical A–π–Pt–π–A skeleton is dispersed uniformly on the whole molecule, whereas the electronic density of the LUMO orbital is mostly located at the two acceptor sides. An obvious

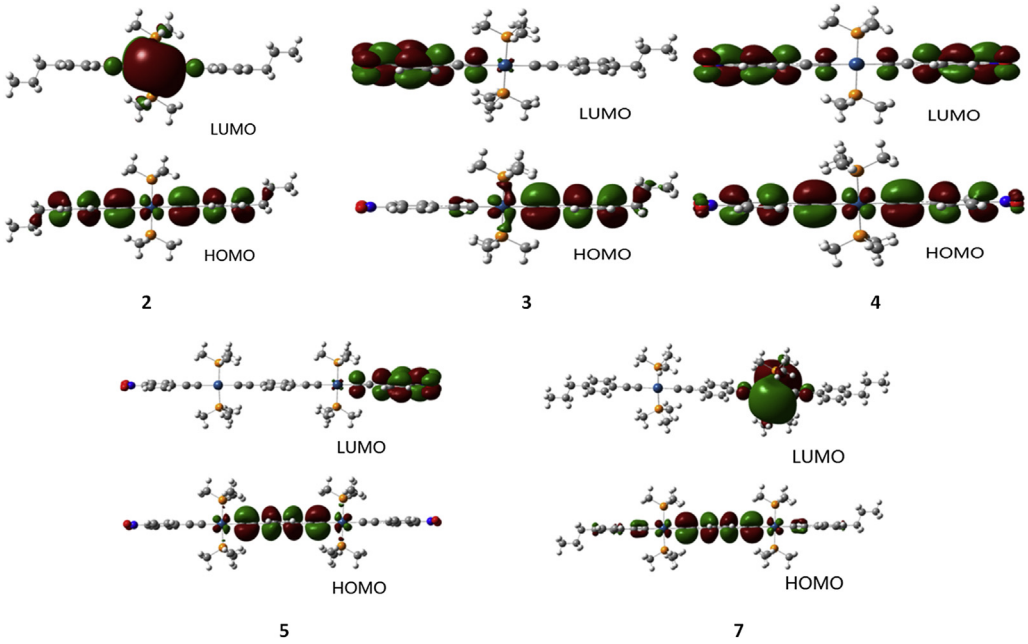

Fig. 2. Electronic density distribution of the HOMO and LUMO orbitals of the platinum acetylides with donor–acceptor structure.

metal-to-ligand charge transfer (MLCT) happens when the molecule is excited, and almost no contribution of the metal d_π involves in LUMO. A similar result is collected for **5**. The platinum acetylides with donor–acceptor structure keep the conjugated system after the insertion of Pt(II) ion into the skeleton of an organic molecule and the electron transfer process could occur by passing through the metal ions. In addition, the charge transfer behavior of these complexes should be dominated by the structure of the molecular skeleton, which makes it possible to study the effect of the insertion of heavy metal ions on the two photon-absorption of the organic molecules with donor-accepter structures.

According to the calculated results listed in Table 1, the energies of the HOMO and LUMO of the complexes decrease when the electron donor is replaced by electron acceptor, this is in accord with the literature [6]. In addition, comparing the orbital energies of **2**, **7**, **4** and **5** indicates that the insertion of the central aryl groups increases the energy levels of HOMO and LUMO, and the energy intervals between HOMO and LUMO decrease at the same time. In addition, the insertion of the central aryl groups makes the electronic density of HOMO more localized on the conjugated ligands with less contribution of the metal d_π. These calculation results are consistent with the reported results by Schanze [18,20].

3.2. Photophysical properties

Fig. 3 shows the electronic absorption spectra of **1**–**8** in chloroform and the data are summarized in Table 2. All the spectra exhibit intense absorption bands from 300 nm to 400 nm, which can be assigned to the $\pi-\pi^*$ transition, and moderate intense absorption bands from 200 nm to 300 nm, which can be assigned to $\pi-\pi^*$ transition of the aryl rings. This observation is consistent with other reports in the literature [20,29]. The weak absorption above 450 nm provides a wide observation window for the application in optical limiter. The absorption maxima of **2** red shifted by 21 nm compared to **1**, which shows that the insertion of Pt(II) ion not only retains but also enlarges the conjugated system of the molecule. For complexes **2**, **7** and **8**, in which two electron donors were connected to the two sides of the molecules, there is a clear red shift in the absorption maxima when the conjugated system of the molecule is enlarged. However, for complexes **4**, **5** and **6**, in which two electron acceptors were connected to the two sides of the molecules, there is no clear red shift in the absorption maxima. Comparison of the absorption spectra of **2**, **3** and **4**, **5** and **7**, **6** and **8**, it can be concluded that replacing the electron donor by electron acceptor can induce the absorption maxima red shift. This is in accord with the calculated results and the literature report [13,18].

Fig. 4a and b presents the luminescence spectra of **1**–**8** in air-free chloroform at room temperature and the emission data are summarized in Table 2. The maxima of the luminescence spectra of **1** and **2** are all located at 374 nm, the emission intensities of them don't change greatly after the N_2 gas was bubbled and the lifetimes are 0.44 ns and 1.47 ns, respectively, which indicate that the emission peaks are the fluorescence. The luminescence spectra of **3**–**8** in air-saturated chloroform display two main peaks. The former peak with shorter wavelength turns weak and the latter peak turns strong in air-free solution (Fig. S17). As shown in Table 1, the lifetimes of former peaks are between 1 and 3 ns and the lifetimes of the latter peaks are between 1 and 6 μs. So the former emission peak can be attributed to the fluorescence and the latter emission peak can be attributed to the phosphorescence. The stokes shift of **1** (59 nm) is much larger than that of **2** (38 nm), which indicates that the insertion of Pt(II) ion decreases the structural rigidity of the molecule and decreases reorganization energy between the ground state and the first singlet excited state. It can be seen from comparison of the Stokes shifts of **2**, **3**, and **4** that replacing the electron donor by electron acceptor can induce the increase of the Stokes shift. For complexes **4**, **5** and **6**, the

Table 1
The calculated energies of HOMO and LUMO of the synthesized complexes.

Complex	1	2	3	4	5	7
LUMO/a.u.	−0.045	0.086	0.041	0.034	0.040	0.087
HOMO/a.u.	−0.205	−0.265	−0.277	−0.311	−0.265	−0.250
ΔE/a.u.	0.160	0.351	0.318	0.345	0.305	0.337

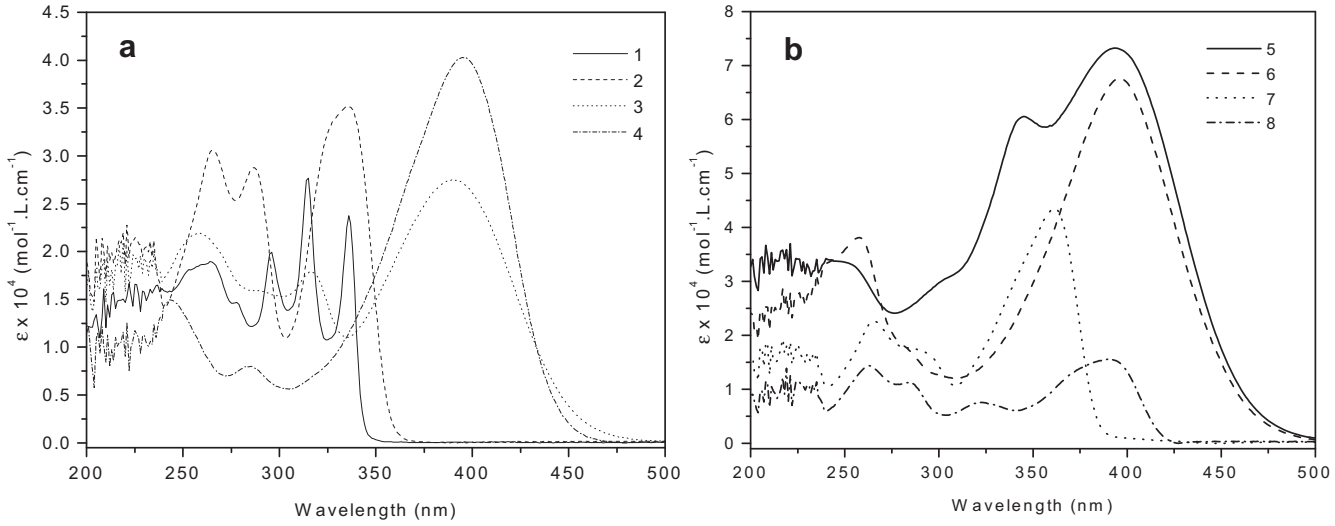

Fig. 3. Electronic absorption spectra of compounds **1**–**8** in chloroform.

insertion of two Pt(II) ions and the central aryl groups induced the decrease of Stokes shift. It is because that the increase of the σ bands in the molecule decease the rigidity of the molecule. In addition, the Stokes shifts increase when the benzyl group was replaced by the naphthanyl group as the central aryl group. It is because that the structural rigidity of the naphthanyl group is greater that of benzyl group. The same conclusion can be drawn from the comparison of the Stokes shifts of **2**, **7**, and **8**. The increase of the Stokes shift also indicates the increase of the reorganization energy between the ground state and the first singlet excited state.

Table 2
Photophysical properties of **1**–**8**.

Compound	λ_{max}/nm	λ_f/nm	Stokes-shift/nm	λ_p/nm	Φ_f	τ_f/ns	τ_p/μs
1	315(2.77 × 10^4)	374	59	–	0.053	0.44	–
2	336(3.52 × 10^4)	374	38	–	0.038	1.47	–
3	390(2.75 × 10^4)	438	48	601	0.017	1.34	1.11
4	395(3.95 × 10^4)	468	73	587	0.016	1.29	5.20
5	394(7.32 × 10^4)	433	39	588	0.045	1.36	3.34
6	396(6.76 × 10^4)	443	47	593	0.030	1.29	1.24
7	361(4.36 × 10^4)	380	19	516	0.041	2.58	1.12
8	390(1.56 × 10^4)	417	27	634	0.029	1.42	1.93

The fluorescence quantum yields (Φ_f) of the synthesized complexes are measured using relative method and the data is listed in Table 2. **1** has the highest Φ_f, which indicates the heavy atom effect decrease the Φ_f because of the increase of the intersystem crossing quantum yield. The increased intersystem crossing quantum yields make it possible for the molecules to possess great triplet excited state absorption. The phosphorescence of the synthesized complexes is seriously overlapped with the corresponding fluorescence, so we do not calculate the quantum yields of the phosphorescence.

3.3. The first-order hyperpolarizabilities

The first-order polarizability (β_{xxx}) of organic molecules can be determined by the solvatochromism method. The simple expression of the first-order polarizability is shown in Eq. (1) [30]:

$$\beta_{xxx}(2\omega) = 3/2\hbar^2\mu_{eg}^2\left(\mu_e - \mu_g\right)\omega_{eg}^2/\left(\omega_{eg}^2 - \omega^2\right)\left(\omega_{eg}^2 - 4\omega^2\right) \quad (1)$$

where ω_{eg} is the frequency of the transition from the ground state to the first excited state, μ_{eg} is the transition dipole moment

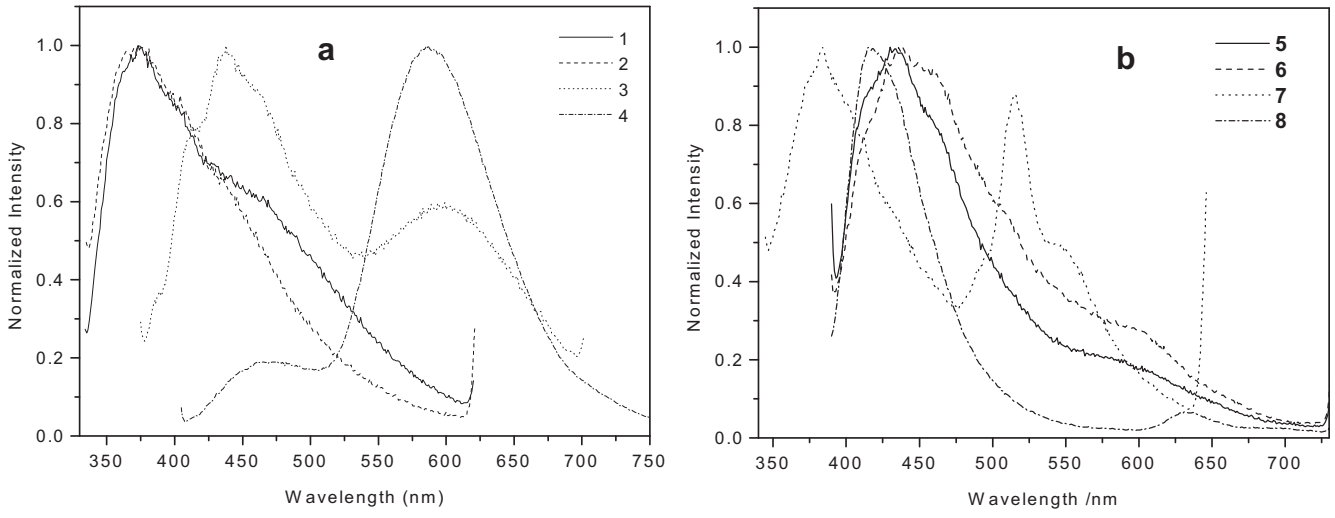

Fig. 4. Luminescence spectra of **1**–**8** in air-free chloroform at room temperature.

Table 3
The data of ω_{eg}, μ_{eg}, $(\mu_e - \mu_g)$ and $|\beta_{xxx}|$ of **1**–**8**.

Compound	ω_{eg} (S^{-1})	μ_{eg} (esu cm)	$(\mu_e - \mu_g)$ (esu cm)	$\lvert\beta_{xxx}\rvert$ (cm^5/esu)
1	5.61×10^{15}	3.27×10^{-17}	3.15×10^{-18}	1.02×10^{-29}
2	5.61×10^{15}	6.02×10^{-17}	3.75×10^{-18}	4.13×10^{-29}
3	4.82×10^{15}	11.2×10^{-17}	7.48×10^{-18}	2.60×10^{-28}
4	4.77×10^{15}	10.2×10^{-17}	3.48×10^{-18}	1.00×10^{-28}
5	4.82×10^{15}	6.19×10^{-17}	1.87×10^{-18}	1.97×10^{-29}
6	4.76×10^{15}	11.0×10^{-17}	2.67×10^{-18}	8.91×10^{-29}
7	4.77×10^{15}	12.0×10^{-17}	4.14×10^{-18}	1.65×10^{-28}
8	5.22×10^{15}	6.65×10^{-17}	2.83×10^{-18}	3.46×10^{-28}

between the ground state and the excited state, μ_g is the permanent dipole moment of the ground state, μ_e is the permanent dipole moment of the excited state, and ω is the laser frequency. ω_{eg} can be found from the absorption band maximum of the title molecule. μ_{eg} can be gotten from the area under the absorption band [31]. The value of $\mu_e - \mu_g$ could be derived from Eqs. (2)–(4).

$$\zeta_a - \zeta_f = A + B(\mathrm{BK}) \tag{2}$$

$$B = 2\left(\mu_e - \mu_g\right)^2 / hca^3 \tag{3}$$

$$(\mathrm{BK}) = \left[(\varepsilon - 1)/(2\varepsilon + 1) - \left(n^2 - 1\right)\Big/\left(2\ n^2 + 1\right) \times \right]\Big/\left[1 - \left(n^2 - 1\right)\Big/\left(2\ n^2 + 1\right)\right]^2 [1 - (\varepsilon - 1)/(2\varepsilon + 1)] \tag{4}$$

where $\zeta_a - \zeta_f$ is the Stokes shift in wave number. a is the radius of a spherical cavity in the solvent occupied by the molecule. ε is the dielectric constant of solvent, n is the refractive index of solvent. BK is the Bilot–Kawski value of the solvent. The parameters of **1**–**8** in five selected solvents are listed in Table 3. The first-order polarizability $|\beta_{xxx}|$ were finally calculated by substituting the values of ω_{eg}, μ_{eg}, and $\mu_e - \mu_g$ into Eq. (1).

From the experimental results, it can be seen that the first-order hyperpolarizabilities of the title complexes are similar to that of the common second-order nonlinear materials *p*-nitroaniline ($|\beta_{xxx}| \sim 20 \times 10^{-30}$ cm^5/esu) and nitro-*N*,*N*-dimethylaniline (37×10^{-30} cm^5/esu) [32]. For complexes **1** to **4**, β_{xxx} of the complexes with symmetrical A–π–Pt–π–A skeleton is larger than that of the complexes with symmetrical D–π–Pt–π–D skeleton, however it is lower than that of the complexes with unsymmetrical D–π–Pt–π–A skeleton. It's probably because of the existence of the symmetric center [33,34]. For complexes **5** to **8**, β_{xxx} of the complexes with symmetrical A–π–Pt–π–Ar–π–Pt–π–A skeleton is smaller than that of the complexes with symmetrical D–π–Pt–π–Ar–π–Pt–π–D skeleton. The first-order hyperpolarizabilities of the title complexes are still impressive although it were not designed based on the criteria for organic second harmonic (SHG) materials.

4. Conclusions

In order to study the detailed relationship between the structure and the two-photon absorption and excited state absorption, as well as whether the two-photon absorption and the excited state absorption of an organic molecule restrain each other, a series of platinum(II) arylacetylides with donor–acceptor structures were synthesized and their photophysical properties were studied systematically. The weak absorption in the visible area of these molecules provides a wide observation window for the application in optical limiter. The calculation using DFT shows that the contribution of the metal d_π in HOMO and LUMO and the charge transfer process are dominated by the skeleton structure of these complexes. The low fluorescent quantum yields and detectable room temperature phosphorescence indicate that the complexes containing Pt(II) have pretty high system-cross quantum yields because of the spin-orbit coupling between the d orbitals of the Pt(II) and the large π-conjugated system. The first-order polarizabilities $|\beta_{xxx}|$ was determined by the solvatochromic method between 1.02×10^{-29} to 3.46×10^{-28} (cm^5/esu). The detailed nonlinear optical properties and the relationship between the structure and properties will be studied soon.

Acknowledgments

The authors thank the Opening Research Foundation from the State Key Laboratory of Laser Interaction with Mater (China) [Grant No. SKILL1005] for the financial support.

Appendix A. Supplementary data

Supplementary data related to this article can be found at http://dx.doi.org/10.1016/j.jorganchem.2013.11.032.

References

[1] H. Sirringhaus, N. Tessler, R.H. Friend, Science 280 (1998) 1741–1744.
[2] S.S. Chavan, B.G. Bharate, Inorg. Chim. Acta 394 (2013) 598–604.
[3] H. Zhang, D.E. Zelmon, L. Deng, H.K. Liu, B.K. Teo, J. Am. Chem. Soc. 123 (2001) 11300–11301.
[4] T.V. Duncan, P.R. Frail, I.R. Miloradovic, M.J. Therien, J. Phys. Chem. B 114 (2010) 14696–14702.
[5] R. Zieba, C. Desroches, F. Chaput, M. Carlsson, B. Eliasson, C. Lopes, M. Lindgren, S. Parola, Adv. Funct. Mater. 19 (2009) 235–241.
[6] F. Dai, H. Zhan, Q. Liu, Y. Fu, J. Li, Q. Wang, Z. Xie, L. Wang, F. Yan, W.-Y. Wong, Chem. Eur. J. 18 (2012) 1502–1511.
[7] H. Kim, B. Cho, Chem. Commun. 2 (2009) 153–164.
[8] G. Zhou, W.-Y. Wong, C. Ye, Z. Lin, Adv. Funct. Mater. 17 (2007) 963–975.
[9] Y. Chen, L. Gao, M. Feng, L. Gu, N. He, J. Wang, Y. Araki, W.J. Blau, O. Ito, Mini-Rev. Org. Chem. 6 (2009) 55–65.
[10] Y. Chen, S. O'Flaherty, M. Fujitsuka, M. Hanack, L.R. Subramanian, O. Ito, W.J. Blau, Chem. Mater. 14 (2002) 5163–5168.
[11] G. Zhou, W.-Y. Wong, D. Cui, C. Ye, Chem. Mater. 17 (2005) 5209–5217.
[12] J. Zhao, W. Wu, J. Sun, S. Guo, Chem. Soc. Rev. 42 (2013) 5323–5351.
[13] G. Zhou, W.-Y. Wong, Chem. Soc. Rev. 40 (2011) 2541–2566.
[14] E. Glimsdal, M. Carlsson, T. Kindahl, M. Lindren, C. Lopes, B. Eliasson, J. Phys. Chem. A 114 (2010) 3431–3442.
[15] F. Guo, W. Sun, Y. Liu, K. Schanze, Inorg. Chem. 44 (2005) 4055–4065.
[16] K. Kim, K. Schanze, Proc. SPIE 6331 (2006) 63310C.
[17] J.E. Rogers, J.E. Slagle, D.M. Krein, A.R. Burke, B.C. Hall, A. Fratini, D.G. McLean, P.A. Fleitz, T.M. Cooper, M. Drobizhev, N.S. Makarov, A. Rebane, K.Y. Kim, R. Farley, K.S. Schanze, Inorg. Chem. 46 (2007) 6483–6494.
[18] G. Zhou, W.-Y. Wong, S. Poon, C. Ye, Z. Lin, Adv. Funct. Mater. 19 (2009) 531–544.
[19] L. Liu, D. Huang, S.M. Draper, X. Yi, W. Wu, J. Zhao, Dalton Trans. 42 (2013) 10694–10706.
[20] W. Wu, J. Zhao, J. Sun, L. Huang, X. Yi, J. Mater. Chem. C 1 (2013) 705–716.
[21] G.A. Crosby, J.N. Demas, J. Phys. Chem. 75 (1971) 991–1024.
[22] J. Van Houten, R.J. Watts, J. Am. Chem. Soc. 98 (1976) 4853–4858.
[23] S. Bräse, J.H. Kirchhoff, J. Köbberling, Tetrahedron 59 (2003) 885–939.
[24] S. Takahashi, Y. Kuroyama, K. Sonogashira, N. Hagihara, Synthesis 12 (1980) 627–630.
[25] K.A. Leonard, M.I. Nelen, L.T. Anderson, S.L. Gibson, R. Hilf, M.R. Detty, J. Med. Chem. 42 (1999) 3942–3952.
[26] R. Cervini, X. Li, G.W.C. Spencer, A.B. Holmes, S.C. Moratti, R.H. Friend, Synth. Met. 84 (1997) 359–360.
[27] G.B. Kauffman, L.A. Teter, Inorg. Synth. 7 (1963) 245.
[28] M.J. Frisch, G.W. Trucks, H.B. Schlegel, G.E. Scuseria, M.A. Robb, J.R. Cheeseman, J.A. Montgomery, T. Vrevenjr, K.N. Kudin, J.C. Burant, J.M. Millam, S.S. Iyengar, J. Tomasi, V. Barone, B. Mennucci, M. Cossi, G. Scalmani, N. Rega, G.A. Petersson, H. Nakatsuji, M. Hada, M. Ehara, K. Toyota, R. Fukuda, J. Hasegawa, M. Ishida, T. Nakajima, Y. Honda, O. Kitao, H. Nakai, M. Klene, X. Li, J.E. Knox, H.P. Hratchian, J.B. Cross, V. Bakken, C. Adamo, J. Jaramillo, R. Gomperts, R.E. Stratmann, O. Yazyev, A.J. Austin, R. Cammi, C. Pomelli, W.J. Ochterski, P.Y. Ayala, K. Morokuma, G.A. Voth, P. Salvador, J.J. Dannenberg, V.G. Zakrzewski, S. Dapprich, A.D. Daniels, M.C. Strain, O. Farkas, D.K. Malick, A.D. Rabuck, K. Raghavachari, J.B. Foresman, J.V. Ortiz, Q. Cui, A.G. Baboul, S. Clifford, J. Cioslowski, B.B. Stefanov,

G. Liu, A. Liashenko, P. Piskorz, I. Komaromi, R.L. Martin, D.J. Fox, T. Keith, M.A. Al-Laham, C.Y. Peng, A. Na-nayakkara, M. Challacombe, P.M.W. Gill, B. Johnson, W. Chen, M.W. Wong, C. Gonzalez, J.A. Pople, Gaussian 03, Revision B05, Wallingford, CT, 2003.
[29] A. Kohler, J.S. Wilson, R.H. Friend, M.K. Al-Suti, M.S. Khan, A. Gerhard, H. Bassler, J. Chem. Phys. 116 (2002) 9457–9464.
[30] M.S. Paley, J.M. Harris, H. Looser, J.C. Baumert, G.C. Bjorklund, D. Jundt, R.J. Twieg, J. Org. Chem. 54 (1989) 3774–3778.
[31] W. Liptay, Angew. Chem. Int. Ed. 8 (1969) 177–188.
[32] T. Carlos, H. Alan, A. Federico, U. Johan, B. Yaneth, C. Olga, S. Humberto, J. Comput. Methods Sci. Eng. 9 (2009) 289–300.
[33] V. Hrobáriková, P. Hrobárik, P. Gajdoś, I. Fitilis, M. Fakis, P. Persephonis, P. Zahradník, J. Org. Chem. 75 (2010) 3053–3068.
[34] T.C.T. Pham, H.S. Kim, K.B. Yoon, Angew. Chem. Int. Ed. 52 (2013) 5539–5543.